



ANP-10294NP
Revision 1

U.S. EPR Reactor Coolant Pump Motor Flywheel Structural Analysis
Technical Report

March 2009

AREVA NP Inc.

(c) 2009 AREVA NP Inc.

Copyright © 2009

**AREVA NP Inc.
All Rights Reserved**

Nature of Changes

Revision 01

Item	Section(s) or Page(s)	Description and Justification
1.	Title Page	Revised revision level and date
2.	Nature of Changes	Added Revision 1 changes
3.	Contents	Revised page numbering as required
4.	3.0	Revised proprietary markings
5.	3.2	Revised proprietary markings
6.	4.0, Fatigue Cycles	Revised proprietary markings
7.	5.1.3	Revised proprietary markings
8.	5.2	Revised proprietary markings
9.	5.3.2	Revised proprietary markings
10.	5.3.3.	Revised proprietary markings
11.	5.3.4	Revised proprietary markings
12.	5.4.4	Revised proprietary markings
13.	Table 5-3	Revised proprietary markings
14.	Table 5-4	Revised proprietary markings
15.	5.4.6	Revised proprietary markings
16.	5.4.7	Revised proprietary markings
17.	5.5	Revised proprietary markings
18.	6.0	Revised proprietary markings

Contents

	<u>Page</u>
List of Tables.....	iv
List of Figures.....	v
Nomenclature.....	vi
1.0 PURPOSE.....	1-1
2.0 REGULATORY ACCEPTANCE CRITERIA FOR FLYWHEEL DESIGN.....	2-1
3.0 DESCRIPTION OF U.S. EPR RCS PUMP MOTOR FLYWHEEL.....	3-1
3.1 Geometric Properties of Flywheel.....	3-4
3.2 Material Properties.....	3-6
4.0 DESIGN LOADS.....	4-1
5.0 ANALYSIS METHODS AND RESULTS.....	5-1
5.1 Stress Analysis.....	5-1
5.1.1 Radial and Tangential Stresses.....	5-1
5.1.2 Results.....	5-4
5.1.3 Acceptance Criteria:.....	5-4
5.2 Fatigue Analysis.....	5-5
5.3 Critical Speed Analysis for Ductile Fracture.....	5-5
5.3.1 Analysis Technique.....	5-5
5.3.2 Method 1: Assuming Total Plastic Deformation of the Flywheel.....	5-6
5.3.3 Method 2: ASME Code, Section III, Appendix F Analysis.....	5-7
5.3.4 Ductile Fracture Ultimate Speed.....	5-9
5.4 Critical Speed Analysis for Non-Ductile Fracture.....	5-10
5.4.1 K_I Solution for Most Plausible Flaws.....	5-10
5.4.2 Fracture Toughness.....	5-12
5.4.3 Plastic Zone Correction Factor.....	5-12
5.4.4 Fracture Mechanics Acceptance Criteria:.....	5-13
5.4.5 Fatigue Crack Growth Analysis.....	5-17
5.4.6 Results.....	5-18
5.4.7 Non-Ductile Failure Analysis and Critical Speed Including the Effect of Fatigue Crack Growth.....	5-18
5.5 Critical Speed Analysis for Excessive Deformation.....	5-19

6.0	CONCLUSION.....	6-1
7.0	REFERENCES.....	7-1

List of Tables

Table 5-1—Stress Intensity Factor Results at Design Speed of $\omega = 157$ rad/sec	5-15
Table 5-2— K_I and K_{cp} as a function of crack size for $\omega = 251$ rad/sec	5-16
Table 5-3—Fatigue Crack Growth Assuming 12 Years Operation	5-18
Table 5-4—Fatigue Crack Growth Assuming 60 Years Operation	5-18

List of Figures

Figure 3-1—U.S. EPR Reactor Coolant Pump.....	3-2
Figure 3-2—Schematic Drawing of Flywheel	3-3
Figure 3-3—Cylindrical Coordinate System	3-5
Figure 5-1—Tangential and Radial Stresses through Flywheel	5-3
Figure 5-2—General Crack Geometry.....	5-11
Figure 5-3—Crack Depth Definition.....	5-11

Nomenclature

Acronym	Definition
ASME	American Society of Mechanical Engineers
FEA	Finite Element Analysis
FSAR	Final Safety Analysis Report
LOCA	Loss of Coolant Accident
NDE	Non-Destructive Examination
RCP	Reactor Coolant Pump
RG	Regulatory Guide
SRP	Standard Review Plan
U	Usage Factors

1.0 PURPOSE

This technical report is being submitted to the NRC in accordance with Regulatory Guide (RG) 1.14 (Reference 1) in support of U.S. EPR FSAR Tier 2, Section 5.4. This technical report summarizes the evaluations performed for the U.S. EPR reactor coolant pump (RCP) motor flywheel design, to verify its conformance to RG 1.14 and Standard Review Plan (SRP) 5.4.1.1 (Reference 2). RG 1.14 provides positions that are acceptable to the NRC to ensure the potential for failures of the flywheels of reactor RCP motors in light-water-cooled nuclear power reactors is minimized.

The following analysis results are included in this report:

- Stress analysis at normal operating and design speed.
- Analysis to predict the critical speed for ductile fracture of the flywheel.
- Analysis to predict the critical speed for the non-ductile fracture of the flywheel (including fatigue crack growth analysis).
- Analysis to predict the critical speed for excessive deformation of the flywheel.

2.0 REGULATORY ACCEPTANCE CRITERIA FOR FLYWHEEL DESIGN

The following regulatory criteria apply to the design of the RCP motor flywheel design as described in this technical report:

- RG 1.14, Revision 1, Regulatory Position C.2, "Design," except C.2.a, which is addressed in the U.S. EPR FSAR.
- SRP Section 5.4.1.1, Acceptance Criterion 2, "Fracture Toughness," and Acceptance Criterion 4, "Flywheel Design," except criterion 4D, which is addressed in the U.S. EPR FSAR.
- American Society of Mechanical Engineers (ASME) Code, Section III, Appendix F-1331, Criteria for Components and NB-3200 for Fatigue Analysis.

In addition to the above criteria, as noted in U.S. EPR FSAR Tier 2, Section 5.4.1.6, the flywheel complies with the requirement of GDC 4, which requires that components important to safety be protected against the effects of missiles.

3.0 DESCRIPTION OF U.S. EPR RCS PUMP MOTOR FLYWHEEL

The flywheel consists of two disks clamped together [] It is connected to the top part of the motor shaft, above the upper bearing, to increase total rotating assembly inertia, as shown in Figure 3-1. Sufficient inertia allows the RCP to continue rotating during power loss, for a sufficient length of time to maintain cooling flow to the reactor core, and prevent hot spots on the reactor fuel elements.

The flywheel is fitted on the shaft by shrink fitting and vertically retained by a large nut at the top of the shaft. Torque is transmitted during operation by three sets of keys described in the following paragraph.



Figure 3-1—U.S. EPR Reactor Coolant Pump

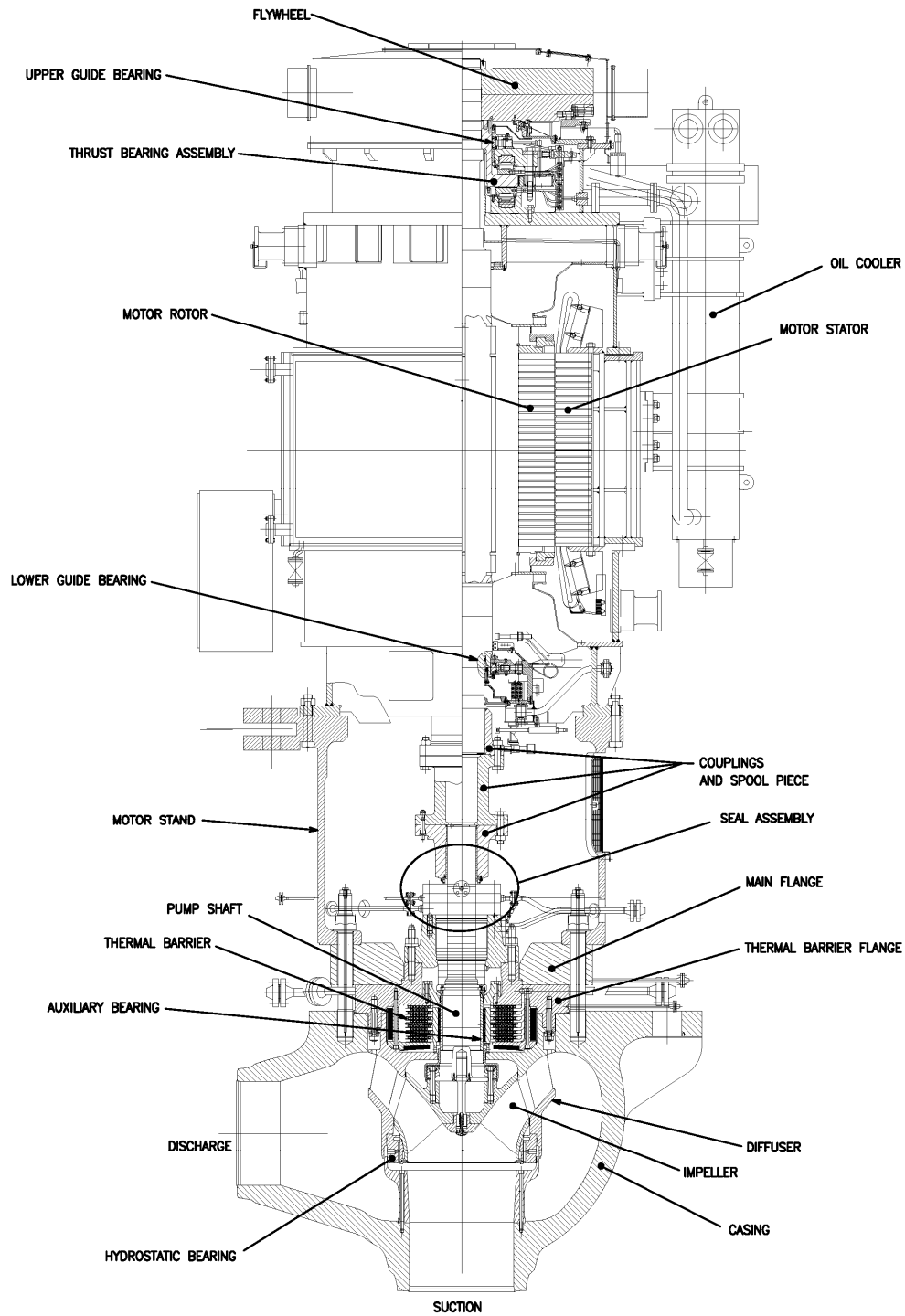
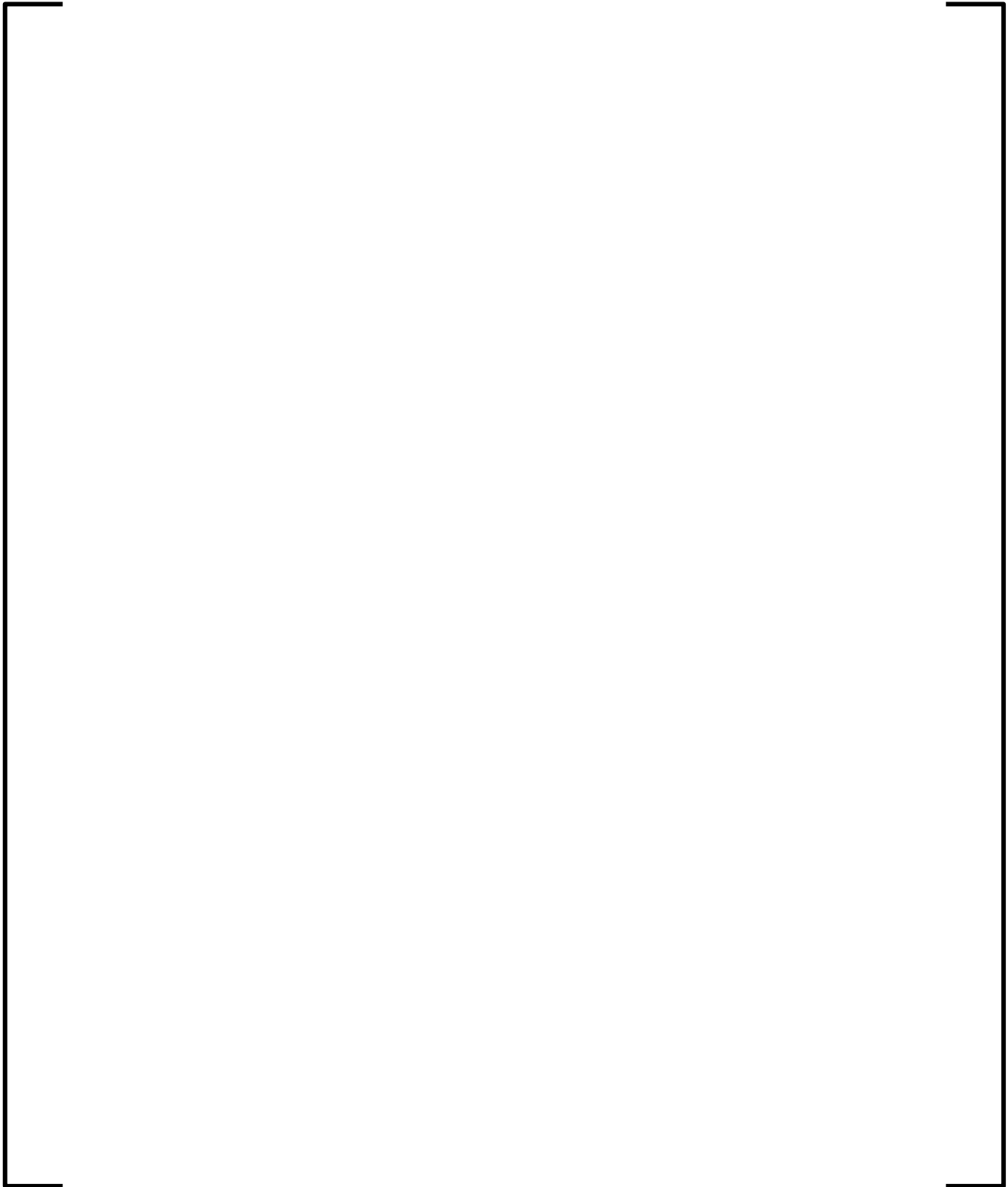


Figure 3-2—Schematic Drawing of Flywheel



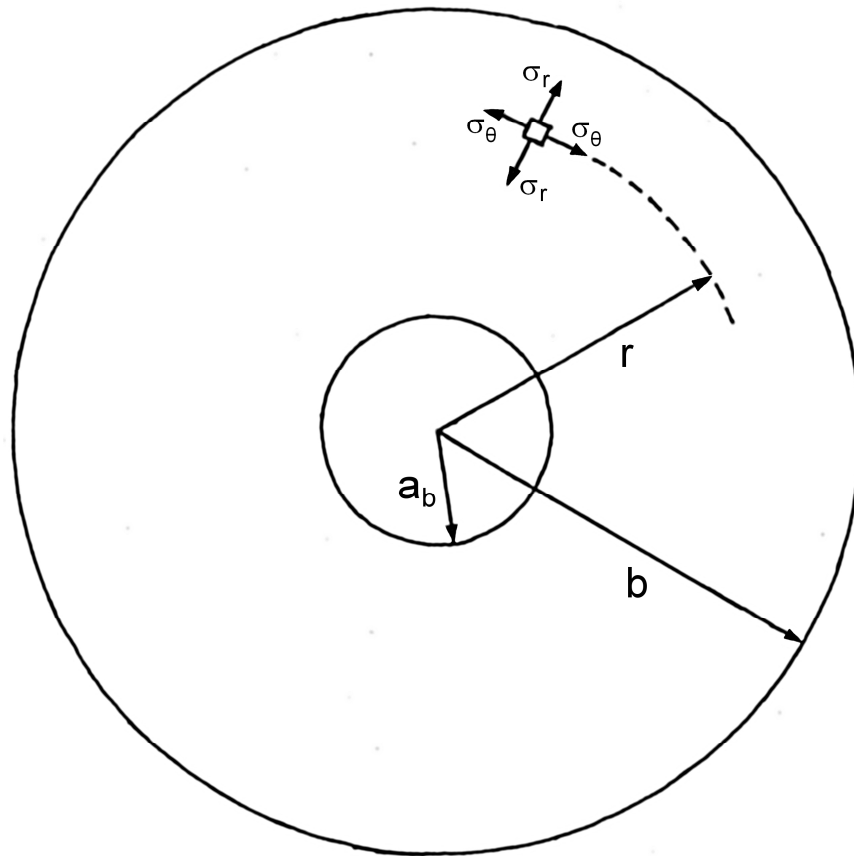
3.1 *Geometric Properties of Flywheel*

The geometric properties of the flywheel are provided below:



Calculations included in this report use a cylindrical coordinate system and variables, as shown in Figure 3-3.

Figure 3-3—Cylindrical Coordinate System



Where:

σ_r	=	Radial stress, psi
σ_θ	=	Tangential stress, psi
b	=	Flywheel outer radius of the lower disk,
in.		
a_b	=	Flywheel inner bore radius, in.
r	=	Flywheel radial location of interest, in.

3.2 **Material Properties**

U.S. EPR RCP motor flywheels are made of SA508 Grade 4N Class 1 – 3½N-1¼Cr-½Mo-V forgings.

Flywheel material properties used in the calculation are shown as follows.

- Young's modulus: $E = 27125 \text{ ksi at } 212^\circ\text{F (187000 MPa at } 100^\circ\text{C)}$
- Poisson's ratio: $\nu = 0.3$
- Material density: $\rho = 0.284 \text{ lb/in}^3 \text{ (7850 kg/m}^3\text{)}$
- Yield stress: $S_y = 79.8 \text{ ksi at } 212^\circ\text{F (550 MPa at } 100^\circ\text{C)}$
- Allowable stress: $S_m = 35 \text{ ksi at } 212^\circ\text{F (241 MPa at } 100^\circ\text{C)}$
- Ultimate Tensile Strength $S_u = 105 \text{ ksi at } 212^\circ\text{F (742 MPa at } 100^\circ\text{C)}$
- Minimum fracture toughness: $K_{IC} = 150 \text{ ksi}\sqrt{\text{in (165 MPa}\sqrt{\text{m)}}$

Thrust Runner:

- Young's modulus: $E = 29007.6 \text{ ksi at } 212^\circ\text{F (200,000 MPa at } 100^\circ\text{C)}$
- Yield stress: $S_y = 84.1 \text{ ksi (580 MPa)}$
- Allowable stress: $S_m = \text{minimum of } 2/3 S_y ; S_u/3 = 37.7 \text{ ksi (260 MPa)}$
- Ultimate Tensile Strength $S_u = 113.1 \text{ ksi (780 MPa)}$

4.0 DESIGN LOADS

The following loading information is for the flywheel analysis.

- Normal operating speed for the flywheel: 1200 rpm
- Design speed: $1.25 \times 1200 \text{ rpm} = 1500 \text{ rpm}$

The highest predicted overspeed is due to a turbine overspeed transient, causing an RCP overspeed of 112 percent of normal operating speed (1344 rpm). The highest predicted overspeed due to loss of coolant accident (LOCA) is less than the highest predicted overspeed due to a turbine overspeed transient. The assumed design overspeed for the analysis was 125 percent of normal operating speed (1500 rpm), in accordance with RG 1.14.

The dimensioning loads are the centrifugal forces (for the flywheel) and the maximum torque C (for the connection between the flywheel and the motor shaft) as shown below:



Therefore, the maximum transient torque applied to the shaft is:

[]

Regarding Other Mechanical Loads

Other mechanical loads not taken into account are listed below because their magnitudes are negligible compared to the maximum transient torque (during the transfer to the stand-by-grid with frequency out of phase).

- Weight loads are negligible.
- Shear stress on the inner radius of the flywheel at maximum transient torque is $< 0.08 \text{ MPa}$, which is negligible.
- Stresses cause by Safe Shutdown Earthquake and LOCA are negligible compared to those caused by centrifugal acceleration, and can be ignored.
- Shrink fit between the flywheel and the shaft need not be considered, as at

nominal speed (1200 rpm) and above, shrink fit is lost, resulting in a [] which reduces loading due to shrink fit to zero. Further information is provided below.

Loss of Flywheel Shrink Fit

The flywheel is shrink fitted onto the motor shaft, which is a negative gap condition of [] maximum. At the normal operating condition of 1200 rpm, centrifugal force causes elastic displacement of the flywheel and the shaft.

The radial displacement due to elastic deformation has been determined using the following equation taken from Timoshenko (Reference 7):

$$\Delta r = r \times \varepsilon_{\theta} = r \times (\sigma_{\theta} - \nu \times \sigma_r) / E$$

Using the flywheel stresses calculated in Section 5.1, the resulting gap at nominal speed (1200 rpm) is:



Fatigue Cycles

A fatigue analysis and crack propagation analysis have been performed using the following duty cycles for a design life of 60 years:

- 4000 start-up / shutdown cycles to normal speed (1200 rpm)
- Included in the 4000 start-up / shutdown cycles are 170 overspeed events from normal speed to 1.10 x normal speed (1320)

The maximum operating time interval between flywheel in-service inspections is expected to be 10 years (Reference 2). For conservatism, this value was extended to 12 years for the flaw growth evaluation summarized in this report.

5.0 ANALYSIS METHODS AND RESULTS

Analyses have been performed to verify conformance with the ASME Codes (References 4 and 5) and the guidance in Reference 1 and Reference 2, in the flywheel design area.

For conservatism, these analyses assumed that the flywheel was a single cylindrical disk with homogenous material and a constant thickness. In actuality, as noted in U.S. EPR FSAR Tier 2 Section 5.4.16.2, the flywheel consists of two circular steel discs mounted on the end of the motor shaft of each RCP. Only centrifugal forces have been applied as loads, as other loads are negligible. Therefore, the stresses in the flywheel are caused by the centrifugal force created by the rotation of the flywheel.

5.1 Stress Analysis

5.1.1 Radial and Tangential Stresses

The radial and tangential stresses are a function of radial distance from the axisymmetric axis (Reference 7).

Given the following assumptions:

- Circular disk with constant thickness
- The stress does not change with the thickness

$$\sigma_{\theta} = \frac{3+\nu}{8} \times \frac{\rho\omega^2}{g_c} \times \left(b^2 + a_b^2 + \frac{a_b^2 b^2}{r^2} - \frac{1+3\nu}{3+\nu} \times r^2 \right)$$

$$\sigma_r = \frac{3+\nu}{8} \times \frac{\rho\omega^2}{g_c} \times \left(b^2 + a_b^2 - \frac{a_b^2 b^2}{r^2} - r^2 \right)$$

Where:

- σ_r = radial stress, psi
- σ_{θ} = Circumferential or tangential stress, psi
- ν = Poisson's ratio
- ρ = flywheel material density, lb/in.³
- ω = flywheel angular speed, radians/sec.
- b = flywheel outer radius, in.
- a_b = flywheel inner radius, in.

Figure 5-1—Tangential and Radial Stresses through Flywheel



5.1.2 Results

Maximum stresses at normal operating speed (1200 rpm)



Maximum stresses at design speed (1500 rpm)



5.1.3 Acceptance Criteria:

In accordance with SRP 5.4.1.1 (Reference 2), Acceptance Criteria II.4.A and II.4.C, the combined stresses at normal operating speed and at the design overspeed should not exceed the following acceptance criteria.

At normal speed (1200 rpm) the required criteria is: $\sigma_{max} < 1/3 \times S_y = 1/3 \times 79.8 \text{ ksi} = 26.6 \text{ ksi}$

- $\sigma_{\theta \text{ max a1}} = 14.46 \text{ ksi}$
- $\sigma_{\theta \text{ max a2}} = 14.48 \text{ ksi}$
- $\sigma_{r \text{ max a1}} = 5.21 \text{ ksi}$
- $\sigma_{r \text{ max a2}} = 4.96 \text{ ksi}$

At design speed (1500 rpm) the required criteria is: $\sigma_{\max} < 2/3 \times S_y = 2/3 \times 79.8 \text{ ksi} = 53.2 \text{ ksi}$

- $\sigma_{\theta \max a1} = 22.59 \text{ ksi}$
- $\sigma_{\theta \max a2} = 22.63 \text{ ksi}$
- $\sigma_{r \max a1} = 8.14 \text{ ksi}$
- $\sigma_{r \max a2} = 7.75 \text{ ksi}$

Therefore, the combined stresses at normal operating speed and design overspeed for the U.S. EPR flywheel are within the acceptance criteria specified in the SRP.

5.2 *Fatigue Analysis*

Based on the detailed calculations and using the ASME Code fatigue curve provided in ASME Code, Section III (Reference 4), usage factors (U) were determined. The results, considering stress concentration factor of three at the edge of the keyway, are:

U = 0.023 for the design life of 60 years and with the fatigue curve $115 < S_u < 130 \text{ ksi}$

U = 0.092 for the design life of 60 years and with the fatigue curve $S_u < 80 \text{ ksi}$

Both usage factors are smaller than 1.0; therefore, the ASME Code fatigue criterion is satisfied.

5.3 *Critical Speed Analysis for Ductile Fracture*

5.3.1 *Analysis Technique*

The critical speed for ductile failure, N_{CRIT} , has been determined by two methods:

1. Assumption of total plastic deformation of the flywheel.
2. Complying with the requirements of ASME Code, Section III, Appendix F-1331.1 (Reference 4).

The minimum value of N_{CRIT} from these two methods has been used, for conservatism.

5.3.2 Method 1: Assuming Total Plastic Deformation of the Flywheel

By applying the Tresca’s criterion, the material begins to deform plastically in the following cases:

1. The shear stress $|\sigma_{\theta} - \sigma_r|/2$ reaches $S_y/2$ or
2. One of the principal stresses reaches S_y .

The second case is applicable here, because both σ_{θ} and σ_r are tensile.

The load limit is reached when the plastic zone extends up to the outer radius of the flywheel ($r = b$), for which we have $\sigma_r = 0$ and $\sigma_{\theta} = S_y$. From this relationship we find

$$\omega_{CRIT} = \sqrt{\frac{S_y g_c}{\rho} \times \frac{3(b - a_b)}{b^3 - a_b^3}} \text{ rad/s} \quad N_{CRIT} = \frac{30}{\pi} \sqrt{\frac{S_y g_c}{\rho} \times \frac{3(b - a_b)}{b^3 - a_b^3}} \text{ rpm}$$

At normal speed of 1200 rpm and at the following radial location from the centerline axis (bore) of the flywheel; tangential and radial stresses were obtained from the stress equations from Section 5.1:

- At $a_b = a_1 = [\quad]$, at the inner bore radius of the lower disk
 $\sigma_{\theta \text{ max}} = [\quad]$
- At $a_b = a_2 = [\quad]$, at the outer radial edge of the keyway
 $\sigma_{\theta \text{ max}} = [\quad]$

Thus, the speed, N_E , for which the stress reaches S_y (elastic/plastic transition speed) is:

$$[\quad] \text{ rpm at inner edge of the bore, } a_b = a_1 = [\quad]$$

$$N_E = 1200 [\quad] \text{ rpm at radial edge of the keyway, } a_b = a_2 = [\quad]$$

Therefore, the critical speed, N_{CRIT} , based on total plastic deformation is:

$$\text{At } a_b = a_1, N_{CRIT} = \frac{30}{\pi} \sqrt{\frac{S_y g_c}{\rho} \times \frac{3(b - a_b)}{b^3 - a_b^3}} = 4105 \text{ rpm.}$$

$$\text{At } a_b = a_2, N_{CRIT} = \frac{30}{\pi} \sqrt{\frac{S_y g_c}{\rho} \times \frac{3(b - a_b)}{b^3 - a_b^3}} = 4057 \text{ rpm.}$$

5.3.3 Method 2: ASME Code, Section III, Appendix F Analysis

By applying Appendix F-1331.1, Section III of ASME Code (Reference 4), the applied primary membrane and primary bending stress intensities have been compared to the material ultimate strength S_U . The stress intensities are acceptable if P_m is less than $0.7S_u$, and $P_m + P_b$ is less than $1.05 S_u$. For each of these criteria a limiting rotational speed is calculated, and the smaller critical speed is used.

The primary membrane and bending stress intensities in a circular disk can be expressed by the following equations:

$$P_m = \frac{1}{(b - a_b)} \int_{a_b}^b \sigma_{\theta} dr \quad P_b = \frac{6}{(b - a_b)^2} \int_{a_b}^b \sigma_{\theta} (r_m - r) dr$$

where the flywheel mean radius is defined as:

$$r_m = \frac{(a_b + b)}{2}$$

Substituting the tangential stress obtained from the stress equations from Section 5.1, yields the following primary membrane and bending load equations in terms of rotational speed and mass density:

$$P_m = \left(\frac{3 + \nu}{8} \right) \times \frac{\rho \omega^2}{g_c (b - a_b)} \times (b^3 - a_b^3) \times \left[1 - \frac{1}{3} \times \left(\frac{1 + 3\nu}{3 + \nu} \right) \right]$$

$$P_b = \left(\frac{3 + \nu}{8} \right) \times \frac{6\rho\omega^2}{g_c (b - a_b)^2} \times [A]$$

$$[A] = \left[\frac{b^4}{12} \times \left(\frac{1+3\nu}{3+\nu} \right) + \frac{b^3 a_b}{2} \times \left[1 - \frac{1}{3} \times \left(\frac{1+3\nu}{3+\nu} \right) \right] - a_b^2 b^2 \ln \left(\frac{a_b}{b} \right) - \frac{b a_b^3}{2} \times \left[1 + \frac{1}{3} \times \left(\frac{1+3\nu}{3+\nu} \right) \right] - \frac{a_b^4}{12} \times \left(\frac{1+3\nu}{3+\nu} \right) \right]$$

- Where:
- P_m = primary membrane stress, psi
 - P_b = primary bending stress, psi
 - ν = Poisson's ratio
 - ρ = flywheel material density, lb/in.³
 - ω = flywheel angular speed, radians/sec.
 - b = flywheel outer radius, in.
 - a_b = flywheel inner radius, in.
 - g_c = gravitational acceleration constant (386.4 in / sec²)

Thus, the primary membrane and bending stress intensities are:

- At the bore radius of lower disk: $a_b = a_1 = [\quad]:$



- At the outer radial edge of the keyway: $a_b = a_2 = [\quad]:$



(where ω is the speed of the flywheel in rad/sec)

The acceptance criteria are as follows:

$$\begin{aligned}
 P_m &< 0.7 Su \\
 &= 0.7 \times 105 \\
 &= 73.5 \text{ ksi (506.8 MPa)} \\
 P_m + P_b &< 1.05 \times Su \\
 &= 1.05 \times 105 \\
 &= 110.25 \text{ ksi (760.2 MPa)}
 \end{aligned}$$

Therefore, the critical speeds based on the ASME Code, Section III, Appendix F criteria are:

- At the inner edge of the bore: $a_b = a_1 = [\quad]$:
 - Based on P_m : 413.4 rad/sec or 3948 rpm
 - Based on $P_m + P_b$: 405.95 rad/sec or 3876 rpm
- At the outer radial edge of the keyway: $a_b = a_2 = [\quad]$:
 - Based on P_m : 408.7 rad/sec or 3903 rpm
 - Based on $P_m + P_b$: 401.2 rad/sec or 3831 rpm

5.3.4 Ductile Fracture Ultimate Speed

Based on the critical speeds determined in Sections 5.3.2 and 5.3.3, the minimum critical speed is;

$$N_{\text{CRIT}} = 3831 \text{ rpm} \quad (\text{at the outer radial edge of the keyway, } [\quad], \text{ based on } P_m + P_b)$$

The safety factor compared to normal speed is:

$$\text{Safety Factor} = \frac{3831}{1200} = 3.19$$

RG 1.14, regulatory position C.2.f states “the normal speed should be less than one-half of the lowest of the critical speeds calculated in regulatory positions C.2.c, C.2.d, and C.2.e above.” As shown above, the normal speed (1200 rpm) is less than one-half of the lowest of the critical speeds (3831 rpm). Therefore, there is a safety factor greater than 2.0, which conforms to the criteria of RG 1.14, regulatory position C.2.f.

Additionally, a finite element analysis (FEA) of the flywheel has been conducted to determine the ductile fracture speed of the flywheel. The results of this analysis, showed agreement between this analytical result of critical speed and the result from the FEA.

5.4 ***Critical Speed Analysis for Non-Ductile Fracture***

The non-ductile fracture mechanics analysis, used to determine the critical speed, includes the following steps:

1. Selection of K_I solution for most plausible flaws.
 - In this analysis a flaw emanating from a hole in a disk is selected in consideration of the maximum stress location as shown in Fig. 5-1.
 - In this analysis a plastic zone size correction r_y is added to the crack size to account for a finite amount of plasticity effect in accordance with Appendix A of ASME Code Section XI.
2. Fracture toughness (K_{Ic}) which should be compared with the applied K_I .
3. Determination of plastic zone correction factor.
4. Fatigue crack growth analysis to determine amount of crack growth due to design cycles.
5. Update calculated applied K_I with the updated crack size and determination of margin in accordance with the acceptance criteria.

5.4.1 ***K_I Solution for Most Plausible Flaws***

The applied force is caused by the centrifugal force due to rotational motion of the disk and the tangential stress on the flywheel is greatest at the inside radius. Therefore, the most likely crack location is shown in Figure 5-2, which is an axial crack emanating from the central hole. In the case of a keyed flywheel, the crack would emanate from the outer radial edge of the keyway, as shown in Figure 5-3.

The approximate solution for the stress intensity factor for a radial crack emanating from the bore of a rotating disk is used, as provided by Reference 8.

Figure 5-2—General Crack Geometry

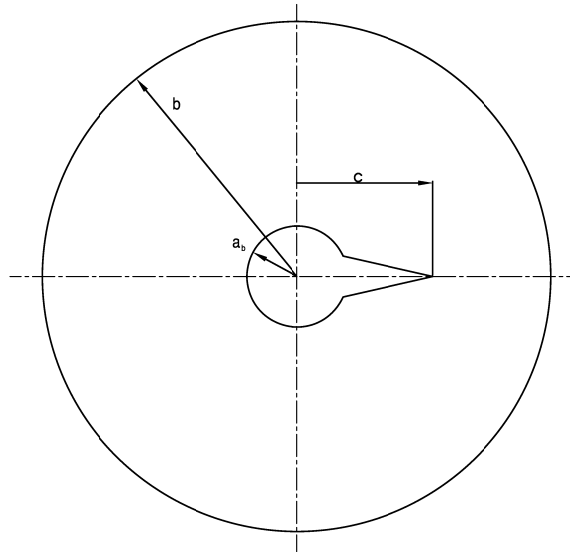


Figure 5-3—Crack Depth Definition



Crack depth, “a,” as used in this report is shown in Figure 5-3, and is defined as:

$$a = c - [\quad]$$

where [\quad] is the distance from the axisymmetric axis to the outer radial edge of the keyway.

$$K_I = \frac{\rho \omega^2}{g_c} \times b^{5/2} \times \phi \times \sqrt{\frac{\pi \times \left(\frac{c}{b} - \frac{a_b}{b} \right)}{1 - \nu^2}}$$

where $\phi = \phi_1 - \phi_2$, and where ϕ_1 and ϕ_2 are defined as:

$$\phi_1 = \frac{3 + \nu}{32} \left\{ \left[3 \times \left(1 + \frac{a_b^2}{b^2} \right) \right] + \left[3 \times \frac{a_b}{b} \times \frac{b}{c} \right] + \left[\left(1 + \frac{a_b}{b} + \frac{a_b^2}{b^2} \right) \times \left(\frac{1 - a_b/b}{1 - c/b} \right) \right] \right\}$$

$$\phi_2 = \frac{1 + 3\nu}{32} \left[\frac{\left(\frac{c}{b} \right)^3 - \left(\frac{a_b}{b} \right)^3}{\frac{c}{b} - \frac{a_b}{b}} + \frac{\left(1 - \frac{a_b}{b} \right)^3}{3 \times \left(1 - \frac{c}{b} \right)} \right]$$

Where:

- ν = Poisson's ratio
- ρ = flywheel material density, lb/in.³
- ω = flywheel angular speed, radians/sec.
- b = flywheel outer radius, in.
- a_b = flywheel inner radius, in. ($a_b = a_1$)
- c = radial location of crack tip, in.
- g_c = gravitational acceleration constant (386.4 in / sec²)

5.4.2 Fracture Toughness

Reference 2 recommends that a minimum value of K_{Ic} is 150 ksi $\sqrt{\text{in}}$. A sample RCP flywheel material has been manufactured and fracture toughness tested in accordance with ASTM E 1820. These tests confirmed that the flywheel material fracture toughness value is greater than the recommended minimum value. However, the smaller value of 150 ksi $\sqrt{\text{in}}$, is conservative; therefore, it was used in the analysis summarized in this report.

5.4.3 Plastic Zone Correction Factor

In accordance with Appendix A to Section XI of the ASME Code (Reference 5), a plastic correction term is added to the analysis to account for crack tip plasticity effect.

K_I is given in Section 5.4.1 for a given crack size a , $K_I(a)$. The plastic zone-corrected K_I , K_{cp} , is given in the following relation:

$$r_y = \frac{1}{6 \times \pi} \times \left[\frac{K_I}{S_y} \right]^2 \qquad K_{cp} = \frac{K_I}{\sqrt{1 - \frac{r_y}{a}}}$$

Where: r_y = plastic zone size, in.
 a = crack size, in.

5.4.4 Fracture Mechanics Acceptance Criteria:

As noted in Acceptance Criterion 4.E of Reference 2, the stress intensity factor with plastic correction K_{cp} must be checked against the following limits:

$$K_{cp} < \frac{K_{IC}}{3.16} \text{ for normal and upset conditions}$$

$$K_{cp} < \frac{K_{IC}}{1.41} \text{ for emergency and faulted conditions}$$

- K_{cp} is applied stress intensity factor (crack driving force)
- K_{IC} is material toughness
- 3.16 is safety factor from ASME Code Section XI for normal and upset condition
- 1.41 is safety factor from ASME Code Section XI for emergency and faulted condition

The minimum fracture toughness of the material (SRP Acceptance Criteria 2) is:

$$K_{IC} = 150 \text{ ksi} \sqrt{\text{in}}$$

For conservatism, the limit for normal and upset conditions is used, thus:

$$K_{cp} < \frac{K_{IC}}{3.16} = 47.5 \text{ ksi} \sqrt{\text{in}} \quad (52.2 \text{ MPa} \sqrt{\text{m}})$$

Comparing the above K_{cp} value to those in Table 5-1 (for design speed), the nearest K_{cp} value in the table corresponds to a final defect size of 1.18 in (30 mm), which is greater

than the recommended value of 0.25 in (6.35 mm) in Reference 2. A factor of 4.72 on crack size, even after a 60 year fatigue crack growth, calculated in Section 5.4.5, is added. See Section 5.4.6 for further conclusions.

In addition, critical crack sizes (safety margin = 1) have been calculated for the following three rotational speeds.

$\omega = 125.6$ rad/sec (1200 rpm):	critical crack depth = 26.02 in (661 mm)
$\omega = 1.25 \times 125.6$ rad/sec = 157 rad/sec (1500 rpm)	critical crack depth = 20.31 in (516 mm)
$\omega = 2 \times 125.6$ rad/sec = 251 rad/sec (2400 rpm):	critical crack depth = 2.32 in (59 mm)

The key stress intensity factor results for $\omega = 2 \times 125.6$ rad/sec for various crack sizes are presented in Table 5-2. The critical crack depths listed above are higher than the critical crack depth of 2.32 in (59 mm).

The calculated ratio of $r_y /$ (crack depth) is [

] at 2 x nominal speed of $\omega = 251$ rad/sec. Therefore the flywheel loading statement is an elastic loading with a confined plastic zone.

Table 5-1—Stress Intensity Factor Results at Design Speed of $\omega = 157$ rad/sec

A large, empty rectangular frame with a black border, intended for the table content. The frame is centered on the page and spans most of the width and height of the page below the caption.

Table 5-2— K_I and K_{cp} as a function of crack size for $\omega = 251$ rad/sec

A large, empty rectangular frame with a thick black border, positioned centrally on the page. It appears to be a placeholder for a table that has not been rendered or is otherwise missing from the document.

5.4.5 Fatigue Crack Growth Analysis

To estimate the magnitude of fatigue crack growth during plant life to material fatigue, the following equations are used, and the most conservative results used. Fatigue crack growth rate is characterized in terms of the range of applied stress intensity factor ($\Delta K_I = K_{\max} - K_{\min}$), and by environmental factors, and can be expressed for carbon and low alloy ferritic steel exposed to an air environment by either of the following equations:

$$\text{Equation 1: } \frac{da}{dN} = 125 \times 10^{-10} \times (\Delta K_I)^3 \text{ mm/cycle}$$

$$\text{Equation 2: } \frac{da}{dN} = 37.8 \times 10^{-10} \times \left(\frac{\Delta K_I}{1 - \frac{R}{2.88}} \right)^{3.07} \text{ mm/cycle}$$

$$\text{Where } R = \frac{K_{I\text{-min}}}{K_{I\text{-max}}}$$

ΔK_I in MPa $\sqrt{\text{m}}$.

Note: Equation 1 - Alternate conservative equation (based on the pump manufacturer vendor experience)

Equation 2 - (ASME Code Section XI, Appendix A-4300, Reference 5)

Crack growth analysis is performed under the cyclic conditions described in Section 4, during a time period corresponding to 12 years (i.e., the conservative time interval between in-service inspections).

Table 5-3 shows the crack propagation values for different initial crack sizes, ranging from 0.25 inch (6.35 mm) and greater after a period of 12 years operation.

Table 5-4 shows the crack propagation values for the minimum crack size of 0.25 inch (6.35 mm) and a period of 60 years operation.

Table 5-3—Fatigue Crack Growth Assuming 12 Years Operation

Initial Crack Size in/mm	Final Crack Size (Equation 1) in/mm	Final Crack Size (Equation 2) in/mm
0.25/6.35	0.2567/6.52	0.2524/6.41
0.3937/10	0.4016/10.20	0.3965/10.07
0.7874/20	0.7984/20.28	0.7917/20.11

Table 5-4—Fatigue Crack Growth Assuming 60 Years Operation

Initial Crack Size in/mm	Final Crack Size (Equation 1) in/mm	Final Crack Size (Equation 2) in/mm
0.25/6.35	0.2839/7.21	0.2626/6.67

5.4.6 Results

None of the values in the above tables exceed the critical value of 2.32 in (59 mm) (where $\omega = 2400$ rpm) given in Section 5.4.4.

The results from Equation 1 are more conservative (bounding), and have been used.

From the postulated initial crack size of 0.25 in (6.35 mm):

- The amount of crack growth is $\Delta a = 0.007$ in (0.17 mm) for the time period of 12 years.
- The amount of crack growth is $\Delta a = 0.034$ in (0.86 mm) for the time period of 60 years.

5.4.7 Non-Ductile Failure Analysis and Critical Speed Including the Effect of Fatigue Crack Growth

The largest flaw which could be missed by inspection is 0.25 in (6.35 mm) in accordance with Reference 2. The expected crack growth for the lifetime of the flywheel (60 design life) is 0.034 in (0.86 mm) as determined in Section 5.4.5.

Therefore, the final crack depth size was assumed to be 0.25 in + 0.034 in = 0.284 in (7.21 mm).

Using this value in the calculations for non-ductile failure of the flywheel results in:

$$\omega = 282 \text{ rad/sec (2693 rpm)} \rightarrow K_{cp} = 150 \text{ ksi}\sqrt{\text{in}}$$

Therefore, the critical speed for non-ductile failure including fatigue crack growth is;

$$N_{CRIT} = [\quad]$$

The safety factor compared to normal speed is:

$$\text{Safety Factor} = \frac{2693}{1200} = 2.24$$

This satisfies the criterion of Reference 1, Paragraph C.2.f.

5.5 **Critical Speed Analysis for Excessive Deformation**

As noted in RG 1.14, excessive deformation during overspeed of the flywheel is of concern because damage could be caused by separation of the flywheel from the shaft. To prevent such a condition, the U.S. EPR has a design feature of a circular collar at the top of the thrust runner, which is positioned to protrude into a ring groove in the bottom of the flywheel. When shrink-fit between the flywheel and the shaft is lost during operation, this collar rides along the inner edge of the groove, which prevents excessive deformation of the flywheel.

The FEA determined that the collar is in contact with the flywheel, at nominal speed and assuming the most conservative initial clearance between the collar and the flywheel of []. The contact pressure between the flywheel and the runner is [] at nominal speed (1200 rpm).

The critical speed for excessive deformation of the flywheel is determined by the allowable stress intensity in the collar, caused by contact with the flywheel. The FEA

provides the following primary membrane and bending stress intensities in the collar at nominal speed:

$$P_m = \quad [\quad]$$

$$P_m + P_b = \quad [\quad]$$

Comparing the above to the allowable stress criteria from ASME Code, Section III, Appendix F-1331.1 (Reference 4), results in P_m being the limiting stress:



Therefore, the critical speed for the collar is:

$$N_{crit} = \sqrt{1200^2 \times \frac{79.2}{9.65}} = 3438 \text{ rpm}$$

The safety factor compared to normal speed is:

$$\text{Safety Factor} = \frac{3438}{1200} = 2.9$$

This satisfies the criterion of Reference 1, Paragraph C.2.f

6.0 CONCLUSION

The U.S. EPR flywheel design conforms to the guidance of RG 1.14 and SRP 5.4.1.1 as summarized below:

1. The lowest critical speed calculated for ductile failure is 3831 rpm. The normal speed of the RCP (1200 rpm) is less than one-half of this speed. This satisfies the guidance of RG 1.14, Paragraphs C.2.c and C.2.f.
2. The lowest critical speed calculated for non-ductile failure is 2693 rpm. The normal speed of the RCP (1200 rpm) is less than one-half of this speed. This satisfies the guidance of RG 1.14, Paragraphs C.2.d and C.2.f.
3. The lowest critical speed calculated for excessive deformation is 3438 rpm. The normal speed of the RCP (1200 rpm) is less than one-half of this speed. This satisfies the guidance of RG 1.14, Paragraphs C.2.e and C.2.f.
4. The lowest overall critical speed is 2693 rpm. The design speed of 1500 rpm, bounds the LOCA overspeed and is less than the lowest all-around critical speed. This satisfies the guidance of RG 1.14, Paragraph C.2.g.
5. As shown in Section 5.1, the combined stresses at normal operating speed do not exceed $1/3$ of the minimum yield strength of the flywheel material. This satisfies the guidance of SRP 5.4.1.1, Paragraph II.4.A for Flywheel Design.
6. As stated in Section 4, the highest predicted overspeed is due to a turbine overspeed transient, causing an RCP overspeed of 112 percent of normal operating speed (1344 rpm). The design speed of the flywheel is 125 percent of normal operating speed which is more than 10 percent greater than the highest predicted overspeed. This satisfies the guidance of SRP 5.4.1.1, Paragraph II.4.B.

7. As shown in Section 5.1, the combined stresses at design speed do not exceed 2/3 of the minimum yield strength of the flywheel material. This satisfies the guidance of SRP 5.4.1.1, Paragraph II.4.C.
8. As shown in Section 5.4.4, using the conservative limit for normal and upset conditions, the ratio of K_{IC} to the K_{cp} at design speed is greater than 3.16 for an initial crack size of 0.25 inches over a 60 year design life. This satisfies the guidance of SRP 5.4.1.1, Paragraph II.4.E.
9. Flaw growth during the 60 year design life of the flywheel including fatigue crack growth due to start-up / shutdown and overspeed cycles was confirmed to be negligible in accordance with the ASME code.

7.0 REFERENCES

1. Regulatory Guide 1.14, "Reactor Coolant Pump Flywheel Integrity," Nuclear Regulatory Commission, August 1975.
2. NUREG-0800, "Standard Review Plan for the Review of Safety Analysis Reports for Nuclear Power Plants," Nuclear Regulatory Commission, March 2007.
3. ASME Boiler and Pressure Vessel Code, Section II, "Materials," American Society of Mechanical Engineers, 2004.
4. ASME Boiler and Pressure Vessel Code, Section III, "Rules for Construction of Nuclear Power Plant Components," American Society of Mechanical Engineers, 2004.
5. ASME Boiler and Pressure Vessel Code, Section XI, "Rules for Inservice Inspection of Nuclear Power Plant Components," American Society of Mechanical Engineers, 2004.
6. R. J. Roark, "Formulas for Stress and Strain," Fifth Edition, McGraw-Hill Book Company, 1975.
7. S. P. Timoshenko and J. N. Goodier, "Theory of Elasticity," Third Edition, McGraw-Hill Company, 1970.
8. J. G. Williams and D. P. Isherwood, "Calculation of the strain-energy release rate of cracked plates by an approximate method," J. of Strain Analysis, Vol. 3, No. 1, pp 17-22, 1968.

U.S. EPR Final Safety Analysis Report Markups

Table 1.6-1—Reports Referenced
Sheet 2 of 4

Report No. (See Notes 1, 2, and 3)	Title	Date Submitted to NRC	FSAR Section Number(s)
ANP-10285P ANP-10285NP	U.S. EPR Fuel Assembly Mechanical Design Topical Report	10/02/07	4
ANP-10286P ANP-10286NP	U.S. EPR Rod Ejection Accident Methodology Topical Report	11/20/07	4.3 and 15
ANP-10287P ANP-10287NP	Incore Trip Setpoint and Transient Methodology for U.S. EPR Topical Report	11/27/07	4, 6, 7, and 15
ANP-10288P ANP-10288NP	U.S. EPR Post-LOCA Boron Precipitation and Boron Dilution Technical Report	12/6/07 (Note 4)	15
ANP-10290	AREVA NP Environmental Report Standard Design Certification	12/6/07 (Note 4)	19.2
ANP-10291P ANP-10291NP	Small Break <u>SBLOCA and Non-LOCA</u> Sensitivity Studies and Methodology <u>Technical Report</u>	12/6/07 (Note 4)	15
ANP-10292	U.S. EPR Conformance with Standard Review Plan (NUREG-0800) <u>Technical Report</u>	12/6/07 (Note 4)	1.9
<u>ANP-10293</u>	<u>U.S. EPR Design Features to Address GSI-191 Technical Report</u>	<u>2/08</u>	<u>15.6.5.4.3</u>
<u>ANP-10294</u> , <u>Revision 1</u>	<u>U.S. EPR Reactor Coolant Pump Motor Flywheel Structural Analysis Technical Report</u>	<u>3/09</u>	<u>5.4.1.6.6</u>
BAW-10132-A	Analytical Methods Description – Reactor Coolant System Hydrodynamic Loadings During a Loss-of-Coolant Accident	7/20/79	App. 3C
BAW-10133P-A BAW-10133-A Revision 1, Addendum 1 and 2	Mark-C Fuel Assembly LOCA-Seismic Analysis	10/30/00	4.2
BAW-10147P-A, BAW-10147-A Revision 1	Fuel Rod Bowing in Babcock & Wilcox Fuel Designs	6/28/83	4.2, 4.4
BAW-10156-A, Revision 1	LYNXT, Core Transient Thermal-Hydraulic Program	8/18/93	4
BAW-10163P-A BAW-10163-A	Core Operating Limit Methodology for Westinghouse Designed PWRs	6/2/89	4.3 and 16

13. ASME “Code for Operation and Maintenance of Nuclear Power Plants,” The American Society of Mechanical Engineers, 2004.
14. ANSI/IEEE Std 603-1998, “IEEE Standard Criteria for Safety Systems for Nuclear Power Generating Stations,” American National Standards Institute/ Institute of Electrical and Electronics Engineers, 1998.
15. EPRI Report 1008219, “EPRI PWR Primary-to-Secondary Leak Guidelines, Revision 3,” Electric Power Research Institute, December 2004.
16. NRC Generic Letter 88-17, “Loss of Decay Heat Removal,” U.S. Nuclear Regulatory Commission, October 17, 1988.
17. SECY 93-087, “Policy, Technical, and Licensing Issues Pertaining to Evolutionary and Advanced Light Water Reactor (ALWR) Designs,” U.S. Nuclear Regulatory Commission, April 2, 1993.
18. SECY 90-016, “Evolutionary Light Water Reactor (LWR) Certification Issues and their Relationship to Current Regulatory Requirements,” U.S. Nuclear Regulatory Commission, January 12, 1990.
19. ANP-10294P, Revision 1 “U.S. EPR Reactor Coolant Pump Motor Flywheel Structural Analysis Technical Report,” March 2009.